

---

01 Jan 2023

## Additively Manufactured Carbon Fiber- Reinforced Thermoplastic Composite Mold Plates For Injection Molding Process

C. Bivens

A. Wood

D. Ruble

M. Rangapuram

*et. al.* For a complete list of authors, see [https://scholarsmine.mst.edu/mec\\_aereng\\_facwork/5405](https://scholarsmine.mst.edu/mec_aereng_facwork/5405)

Follow this and additional works at: [https://scholarsmine.mst.edu/mec\\_aereng\\_facwork](https://scholarsmine.mst.edu/mec_aereng_facwork)



Part of the [Aerospace Engineering Commons](#), and the [Mechanical Engineering Commons](#)

---

### Recommended Citation


C. Bivens et al., "Additively Manufactured Carbon Fiber- Reinforced Thermoplastic Composite Mold Plates For Injection Molding Process," *Applied Composite Materials*, Springer, Jan 2023.

The definitive version is available at <https://doi.org/10.1007/s10443-023-10138-4>

This Article - Journal is brought to you for free and open access by Scholars' Mine. It has been accepted for inclusion in Mechanical and Aerospace Engineering Faculty Research & Creative Works by an authorized administrator of Scholars' Mine. This work is protected by U. S. Copyright Law. Unauthorized use including reproduction for redistribution requires the permission of the copyright holder. For more information, please contact [scholarsmine@mst.edu](mailto:scholarsmine@mst.edu).



# Additively Manufactured Carbon Fiber- Reinforced Thermoplastic Composite Mold Plates for Injection Molding Process

C. Bivens<sup>1</sup> · A. Wood<sup>1</sup> · D. Ruble<sup>1</sup> · M. Rangapuram<sup>1</sup> · S. K. Dasari<sup>1</sup> · K. Chandrashekhara<sup>1</sup>  · J. DeGrange<sup>2</sup>

Received: 20 December 2022 / Accepted: 12 May 2023  
© The Author(s), under exclusive licence to Springer Nature B.V. 2023

## Abstract

Polymer injection molding processes have been used to create high-volume parts quickly and efficiently. Injection molding uses mold plates that are traditionally made of very hard tool steels, such as P20 steel, which is extremely heavy and has very long lead times to build new molds. In this study, composite-based additive manufacturing (CBAM) was used to create mold plates using long-fiber carbon fiber and polyether ether ketone (PEEK). These mold plates were installed in an injection molding machine, and rectangular flat plates were produced using Lustran 348 acrylonitrile butadiene styrene (ABS). Tensile and flexural testing was performed on these parts as well as parts produced using traditional P20 steel mold plates with the same geometry to compare the performance of the different mold plates. The parts produced using the carbon fiber mold plates were within 5% of the tensile strength and 10% of the flexural strength of the traditionally manufactured parts. However, the parts produced using the carbon fiber mold plates required additional cooling time due to the lower conductivity of the carbon fiber composite compared to the P20 steel. This allows additively manufactured composite molds to be a good substitute for conventional molds in low-volume injection molding production.

**Keywords** Injection molding · Additive manufacturing · Thermoplastic · Carbon fiber · Composite material · Polymer

## 1 Introduction

In 2021, the plastics industry produced nearly \$400 billion in global shipments and accounted for 1 million jobs in the United States alone [1]. Over 30% of this market is made up of injection molding alone. Injection molding is used in many high-volume, high-speed applications of thermoplastic, elastomer, and thermoset materials. Additives such as colorants or fillers can also be added to improve mechanical or cosmetic properties. The injection molding process is very robust and provides many advantages such as high dimensional control over

---

✉ K. Chandrashekhara  
chandra@mst.edu

<sup>1</sup> Department of Mechanical and Aerospace Engineering, Missouri University of Science and Technology, Rolla, MO 65409, USA

<sup>2</sup> Impossible Objects Inc, Northbrook, IL 60062, USA

complex geometries, high repeatability, low labor, and low scrap [2]. The injection molding process begins with small pellets of the base material and subjects them to 5 basic steps: plasticizing, injection, filling, cooling, and release [3]. Plasticizing intakes the raw pellets and uses conduction from a series of heaters along with friction from a rotating screw pushing the pellets along the wall of the barrel to fully melt the polymer to the required injection temperature. During injection, a clamping unit closes the mold. Then, a ram forces a pre-set volume of molten polymer into the mold cavity at high pressure. During filling, the screw is held in a forward position to force more polymer into the mold to account for shrinkage due to cooling or small displacements in the machinery. The fourth step, cooling, extracts latent energy from the molten polymer to allow it to solidify in the mold. This step is usually the longest in the process, and also the most important because without uniform cooling, thermal stresses and warping can be induced in the part. Finally, during ejection, the mold is opened, and pins eject the finished part from the mold. The screw retracts to fill a new shot of polymer for the next cycle, and the process can be repeated [4].

One of the biggest drawbacks of conventional injection molding is that it requires extremely high upfront tooling costs. Due to the high precision, complex CNC manufacturing required, simple, small molds often cost \$5,000 with larger, more complex molds costing up to \$100,000 [5]. Additionally, traditional steel molds often have lead times of multiple months and are difficult to repair if the initial design necessitates modification after first article testing, which hampers the economic viability of the injection molding process [6]. Due to these drawbacks, new rapid tooling production methods using additive manufacturing are being considered to produce customized parts with complex geometries, reducing mold production costs and cycle times [7].

Other attempts have been made to create mold plates using various additive manufacturing methods, such as stereolithography, PolyJet 3D printing, and fused filament fabrication (FFF) methods [8]. In 2022, Gohn et al. utilized a desktop extrusion 3D printer to create mold plates for injection molding using both neat polyamide 6 (PA6) nylon and PA6 nylon filled with 12.5% continuous-strand carbon fiber. Even with 100% infill, this process still led to catastrophic degradation of the mold within 15 cycles [9]. Krizsma et al. utilized Stratasys FullCure 720 epoxy-acrylate to build mold inserts with embedded strain gauges and thermocouples to allow in-situ monitoring. It was found that these mold inserts built-up residual strain, which ultimately led to failure within 12 cycles. However, the sensors produced failure warnings in the cycle ahead of the failure [10]. In 2019, Jahan et al. utilized metal powder bed fusion to build mold injection mold cores with topology-optimized cooling channels out of maraging steel and then compared the cooling performance to that of a traditional injection molding core. It was found that the additively manufactured core provided substantially greater cooling performance than the traditional one. However, the quality of the parts manufactured with this method is still being evaluated [11].

In this study, composite-based additive manufacturing (CBAM) was used to create injection molding plates. Composites are primarily composed of fiber material embedded within a matrix. The fibers provide high strength and stiffness to the part necessary to overcome the high clamping and injection pressures. The matrix serves to transfer the load to the fibers, assist in maintaining the part's geometry, and is responsible for the surface finish of the composite mold plates [12]. CBAM creates parts with very low void content and can use a wide range of high-performance long-fiber materials to create extremely high mechanical performance. Furthermore, CBAM takes advantage of additive manufacturing in which highly complex geometries can be quickly created at an affordable cost. In addition, CBAM mold plates can also be designed and adapted to existing dies, thereby reducing production time and costs [13]. The purpose of this study is to evaluate the use of CBAM in the manufacture of injection molding plates for either rapid, functional

prototyping applications or small-run applications. Due to its quick manufacturing times, relatively low cost, and high strengths, CBAM is an excellent candidate to address the shortcomings of conventionally manufactured injection molding plates.

## 2 Manufacturing and Installation of Mold Plates

### 2.1 CBAM Process

The CBAM mold plates used in this study were developed using the CBAM 2 printer, which is manufactured and managed by Impossible Objects Inc. in Northbrook, IL. This process utilizes three main steps in order to produce the final parts from an initial CAD model. First, long-strand carbon fiber veils are taken into the machine. Then a thermal inkjet is used to print an aqueous fluid at 600 dpi on the non-woven composite veils in locations where the final part will be produced. The veils are then passed under a flow of thermoplastic polymer powder which sticks to where the aqueous fluids were printed followed by excess outside the printed region being vacuumed off and recycled. The polymer deposition is done at room temperature so there is no thermal effect on the powder. Each veil is then stacked to create a full build block. This build block is then heated to the melting point of the polymer and then pressed at 150psi (1.03 MPa) which flows the polymer throughout the printed regions of the fiber sheet and fuses the sheets into a solid shape. The final step is using a mechanical blasting process to abrade the un-fused carbon material that is not bound to the PEEK matrix [14]. A summary of this process is presented below in Fig. 1. The material properties of the final CBAM/PEEK composite are shown in Table 1 below [15, 16].

CBAM process can additively manufacture high-strength carbon fiber composites. CBAM is nearly 10 times faster than continuous fiber placement [17]. The other common technique for additively manufactured carbon fiber utilizes chopped fiber, this technology utilizes short fibers randomly scattered throughout the matrix [18]. The longer fibers (0.5–1 in./ 12.5–25 mm) utilized by CBAM increase the stiffness, strength, and toughness of the finished part considerably. CBAM is currently being employed in the automotive industries for weight reduction, defense for rapid manufacturing of high-strength parts, and in industrial applications for tooling and functional prototyping.

### 2.2 CBAM Mold Plate Dimensions and Installation

In this study, a set of mold plates were created using the CBAM process such that, the final injection molded part's shape is a rectangular prism with dimensions of 9.813 inches (249.3 mm) in length, 5.188 inches (131.8 mm) in width, and 0.125 inches (3.2 mm) in depth. with a 0.25-inch (6.4 mm) fillet on each corner. After the CBAM process was complete, standard mechanical subtractive processes were used to finish creating the composite molds. Subtractive processes include drilling of two holes through the mold in order to insert cooling lines, along with five holes for ejector pins within the mold cavity. Due to the compression stage of the CBAM process, creating long, straight, internal passageways are difficult to remove the unfused fibers with current technologies, hence the need for modifications. The mold plates were installed on the dies using the same screws and holes as the steel molds. The final CBAM mold plates mounted to the steel dies are shown in Fig. 2.

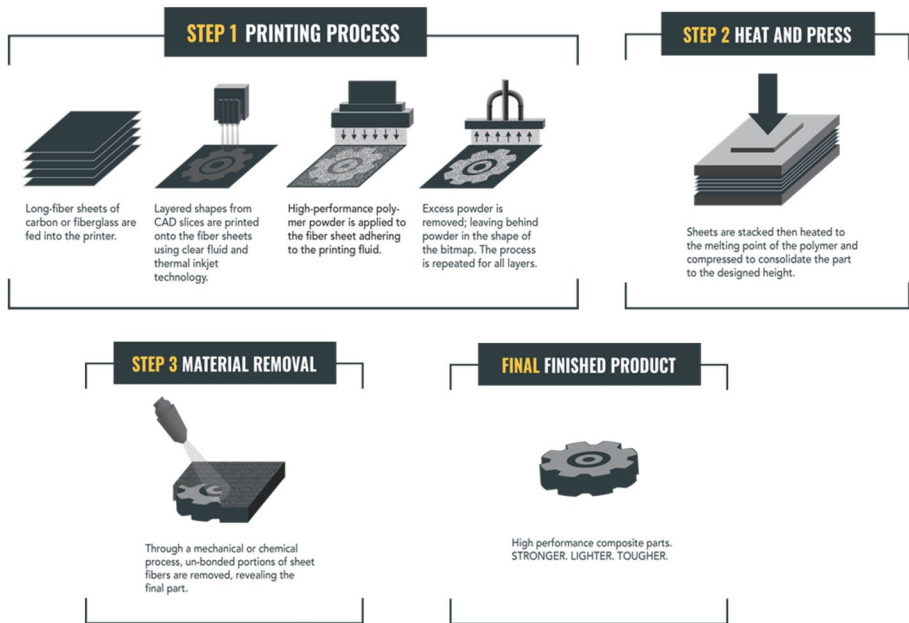


Fig. 1 Summary of the CBAM Manufacturing Process [13]

### 2.2.1 Advantages of CBAM Mold Plates

The CBAM process has several advantages over other methods of creating injection molding plates. Mold plates can be fabricated extremely quickly with the CBAM method. For example, these molds took a total of 26 h to produce: 12 h to print, 12 h to heat and consolidate, and a final 2 h of post-processing time.

In part due to this time reduction, the CBAM mold plates are significantly cheaper to fabricate than comparable steel molds. The estimated cost of CBAM molds is less than 15% of the cost of a comparable steel mold. This reduction in price makes a significant difference to the final cost of products running with a small production cycle.

There is a wide range of materials available for the CBAM process. Currently, long-fiber (fiber length  $\geq 12$  mm) glass and carbon fibers are available with a range of polymer materials. These materials allow for the customization of material characteristics to the

**Table 1** Carbon Fiber/PEEK CBAM Properties

Carbon Fiber/PEEK CBAM Properties		
Density	0.0506 (1400)	lb/in <sup>3</sup> (kg/m <sup>3</sup> )
Tensile Strength	19.1 (132)	ksi (MPa)
Compressive Strength	23.5 (162)	ksi (MPa)
Elastic Modulus	1848 (12.7)	ksi (GPa)
CTE, xy-linear	7.0 (12.6)	$\mu\text{in/in-}^\circ\text{F}$ ( $\mu\text{m/m}^\circ\text{C}$ )
CTE, z-linear	36.4 (65.52)	$\mu\text{in/in-}^\circ\text{F}$ ( $\mu\text{m/m}^\circ\text{C}$ )
Thermal Conductivity	0.16 (0.27)	BTU/hr-ft- $^\circ\text{F}$ (W/ m $^\circ\text{K}$ )

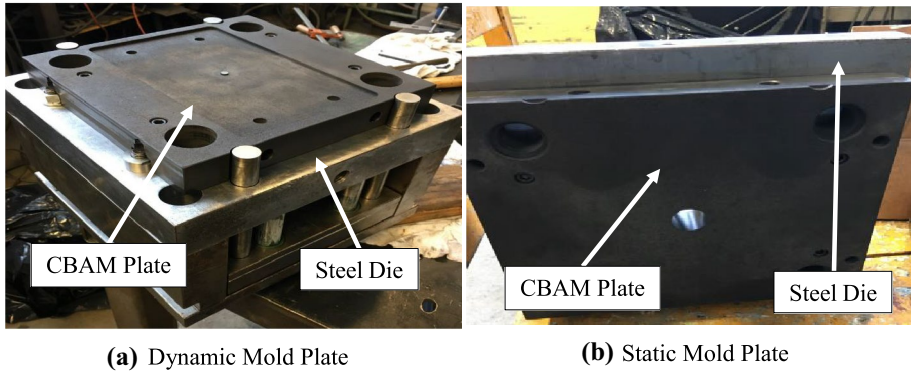


Fig. 2 CBAM Mold Plates attached to Injection Die

application. In this study, carbon fiber/PEEK was used due to its high strength and thermal stability. This also created significant weight savings over the steel molds. The CBAM-produced molds have a density of 0.05 lb/in<sup>3</sup> (1384 kg/m<sup>3</sup>) while P20 steel has a density of 0.284 lb/in<sup>3</sup> (7861 kg/m<sup>3</sup>). This equated to a weight savings of over 80%.

### 2.3 P20 Steel Mold Plates

As a control group, standard steel mold plates with the same geometry were procured. These mold plates were produced using CNC milling of AISI P20 steel. Due to its strong resistance and ability to maintain hardness and strength at high temperatures, AISI P20 steel is one of the most widely used types of tool steel utilized in the plastics injection molding industry [17]. The material properties of the steel mold are listed in Table 2 [19].

One of the most important things about the P20 steel molds is a comparison in the thermal conductivity of the steel compared to the carbon fiber/PEEK. The steel has a very high thermal conductivity of 24 BTU/(hr-ft-°F) (0.91 W/(m<sup>2</sup>-°C)), as shown in multiple data sheets from tool steel corporations [19]. The thermal conductivity for the carbon fiber/PEEK mold material is significantly lower with a value of 0.16 BTU/(hr-ft-°F) (136 W/(m<sup>2</sup>-°C)). This means that heat is transferred to the steel molds at a rate approximately 150 times faster than that of the composite molds. This entails significantly longer cooling times for parts created within composite molds. However, CBAM mold plates are substantially cheaper to manufacture [20].

Table 2 P20 Steel Properties

P20 Steel Properties		
Density	0.284 (7861)	lb/in <sup>3</sup> (kg/m <sup>3</sup> )
Brinell Hardness	300	-
Tensile Strength	125 (861)	ksi (MPa)
Compressive Strength	125 (861)	ksi (MPa)
Elastic Modulus	29,700 (205)	ksi (GPa)
CTE, linear	7.1 (12.78)	μin/in-°F (μm/m°C)
Thermal Conductivity	24 (41.50)	BTU/hr-ft-°F (W/ m°K)

### 3 Manufacturing of ABS Parts and Process Modifications

The injection molding process uses thermal processes to melt a thermoplastic polymer, inject the molten polymer at high pressure into a mold, cool the polymer to a hard solid, and then eject the completed part from the mold.

#### 3.1 Injection Molding Material

For this study, Lustran 348 Acrylonitrile Butadiene Styrene (ABS) was selected as the material of interest for injection molding. The material used in this study was supplied by Avient in Avon Lake, OH. The material specifications can be found in Table 3 [20]. ABS is a non-toxic amorphous polymer consisting of three monomers: acrylonitrile, butadiene, and styrene [21]. The amorphous polymer has properties like high rigidity and impact resistance, along with high dimensional stability [22]. ABS is commonly used in the manufacturing of LEGO toys, as well as other applications, such as medical, automotive, consumer electronics, and other industries [23]. ABS was chosen due to high supply availability, easy processability, and because it is widely utilized throughout many applications of injection molding.

#### 3.2 Setup and Process Modifications

##### 3.2.1 Mold Tonnage

The tonnage in injection molding refers to the amount of force applied by the machine to the mold plates when they are clamped together. The clamping pressure multiplied by the part area in the mold must not exceed the tonnage of the injection molding clamp in order to prevent damage to the molds and to maintain dimensional control of the plastic parts [24]. If the tonnage is too low, the injection pressure will induce excess flashing, creating sharp edges on the part. The maximum allowable tonnage is a function of the mold's compressive strength and surface area of the mold as shown in Eq. (1).

$$P_{max} = \frac{\sigma_c \cdot (SA)}{2000 \text{ lbs}} \quad (1)$$

Applying this to the CBAM mold, it is found that the maximum allowable tonnage is 483 tons which, although lower than the steel mold, is still vastly higher than the injection molding machine's maximum of 165 tons. The minimum tonnage required for a mold is estimated by the following equation where  $K_p$  is the clamping force constant based on the material being injected, SA is the surface area of the part, and SF is a safety factor.

**Table 3** Lustran 348 ABS Material Properties

Lustran 348 ABS Material Properties		
Density	0.038 (1051.84)	lb/in <sup>3</sup> (kg/m <sup>3</sup> )
Melt Temperature	475–525 (246–274)	°F (°C)
Shrinkage	4.0E-3 to 6.0E-3	in/in (m/m)
Drying Temperature	175 (79)	°F (°C)
Drying Time	At least 2 h	
Mold Temperature	85–140 (29–60)	°F (°C)

$$P_{min} = K_p \cdot SA \cdot SF \quad (2)$$

Lustran 348 ABS was used in this study which has a  $K_p$  of 1.2. This results in a minimum tonnage of 55 tons, therefore, the CBAM mold and injection molding machine are strong enough to withstand the required tonnage for this mold. For this study, the maximum injection molding machine's allowable tonnage (165 tons) was used for all trials.

### 3.2.2 Cooling Systems and Times

Cooling is a critical step in the injection molding process. Traditionally, over half of the cycle time is spent in the cooling stage. The cooling time gives the molten part time to transfer thermal energy from the mold, thus solidifying the final geometry and mechanical properties before the part is ejected from the mold [24].

Traditionally, cooling systems for injection molding utilize a cooling fluid that flows through pipes to the mold, and then back to a thermal processing unit. Usually, this cooling fluid is water that is channeled via metal piping through the mold. The fluid then comes into direct contact with the mold plates via internally bored cooling channels and exits via metal piping outlets. This allows convection of latent energy from the mold into the water. This water is maintained at a temperature between 100 and 120 °F (38–49 °C) depending on a variety of factors to avoid warpage due to high thermal gradients [25]. Unlike steel, CBAM products have a slightly porous surface finish. Due to this, the CBAM mold plates cannot be directly exposed to the cooling fluid, or else the finished part quality would be diminished. In this study, copper tubing was run through the molds to carry the water. The tubing chosen had an outside diameter of 0.5 in (12.7 mm), a wall thickness of 0.049 in (1.25 mm), and an inside diameter of 0.375 in (9.53 mm). Copper was chosen due to its high thermal conductivity (400 BTU/(hr-ft-°F) (2271 W/(m<sup>2</sup>-°C)), high melting point, and low thermal expansion. Furthermore, carbon and copper have very similar electro potentials meaning that galvanic corrosion is unlikely.

Cooling time is also an important factor to consider in the process. Without enough cooling time, the part will not be solidified when it is ejected from the mold, thus leading to warpage and surface delamination. Contrarily, cooling too fast may induce residual stresses within the mold leading to warping effects and weak structural rigidity. The following equation is used to estimate the required cooling time using a steel mold:

$$T_{Cooling} = \frac{d_{sprue}^2}{\pi^2 \alpha} \ln \left( \frac{4(T_M - \bar{T}_W)}{\pi(\hat{T}_E - \bar{T}_W)} \right) \quad (3)$$

where  $d_{sprue}$  is the sprue diameter,  $\alpha$  is the coefficient of thermal diffusivity of the molten polymer,  $T_M$  is the injection temperature of the molten plastic,  $\bar{T}_W$  is the average temperature of the mold plate surface, and  $\hat{T}_E$  is the average temperature of the part when it is ejected from the mold [26]. When applied to the steel mold, this results in approximately 10 s of cooling time. However, the CBAM material has far lower thermal conductivity than the steel does, and as such, the mold surface temperature absorbs heat from the polymer slower. Through experimentation performed in [27], it was found that 60–90 s of cooling time was necessary to fully transition the part to an amorphous solid both of which were applied to this study.

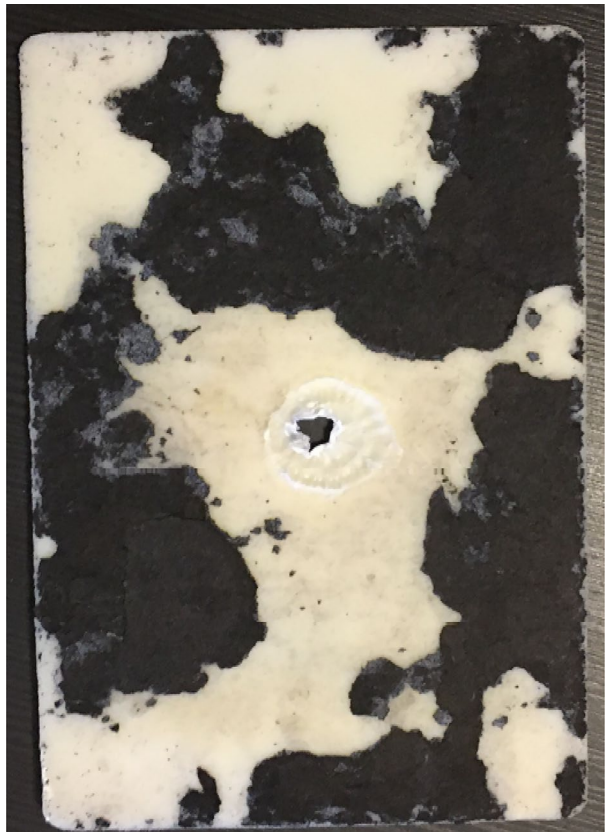


### 3.2.3 Modifications to CBAM Mold Plate

As a further result of the poor surface finish of the mold plate, an impervious coating had to be applied to the surface of the mold. Initially, a conventional two-part mold sealant/release system was attempted. After the first part was made, it was found that this system was insufficient to properly prevent the liquid polymer from adhering to the surface of the CBAM mold as shown in Fig. 3. The black splotches are areas where the plastic had adhered so much to the mold that in order to remove the part, the mold delaminated.

The mold had to be repaired by using a float to spread a thin layer of J-B Weld steel-reinforced epoxy to restore a smooth surface finish. This material was selected due to its similar thermal conductivity to the CBAM material, as well as its ability to withstand the high temperatures and pressures encountered in the injection molding process. Once the mold was repaired, a new system to protect the mold plates was proposed. In this system, a high-temperature, 0.004 in (0.1 mm) thick, metallic-backed tape was applied to all surfaces the plastic would come in contact with. This tape creates a better surface finish which allows for the mold release to stay in contact with the plastic rather than sinking into the CBAM mold. Although this might improve the surface finish over the as-printed tooling part, thermal effects are considered negligible due to the extremely low thermal mass. This newly protected mold is shown in Fig. 5, along with the first couple of parts made with

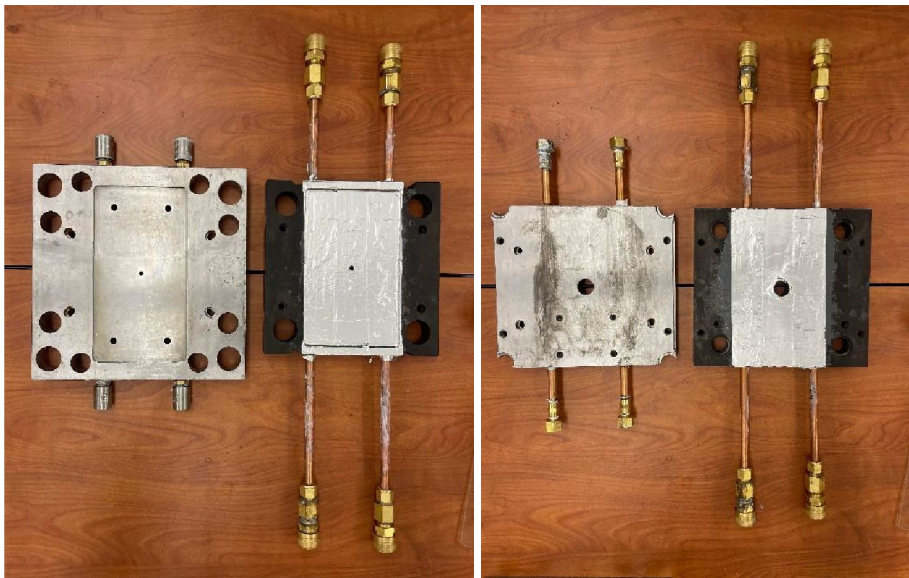
**Fig. 3** Injection Molded Part using Mold Release



those molds shown in Fig. 4. After visual inspection (no magnification), these parts looked to be free of cracks, fully filled the mold, and removed cleanly, so this tape system was used for all remaining trials with the CBAM-manufactured mold plates. Throughout the study, over 30 parts were made with this mold protection system with no noticeable degradation of quality.

### 3.3 Manufacturing

For this study, a Cincinnati Milacron VT-165 165-ton injection molding machine at the Missouri University of Science and Technology's Composite Manufacturing Laboratory is used. Parts were manufactured with both the steel mold and the CBAM mold before cutting out test articles for tensile and flexural testing. Due to the hygroscopic nature of ABS, before inserting the pellets, they were dried in an industrial dryer at 180 °F (82.2 °C) for at least 9 hours per the technical datasheet. The injection molding machine used has a three-banded heater screw along with a heated sprue. The rear band was set to 465 °F (240 °C), the mid to 475 °F (246 °C), and the front was set to 485 °F (252 °C). The sprue was also set to 485 °F (252 °C) which maintains the temperature of the molten plastic in the mold. Once reaching the designated operating temperature, the machine was allowed to "soak" at this temperature for 30 minutes before parts began being manufactured. For all parts made in the steel mold, the cooling time was set to 10 seconds. Parts for tensile testing specimens made in the CBAM mold were cooled for 90 seconds. Flexural testing specimens were cooled for either 30, 60, or 90 seconds to compare the effect of cooling time on the material performance and to find a cooling time at which



(a) Dynamic Mold Plates

(b) Static Mold Plates

**Fig. 4** Comparison of Steel and Protected CBAM mold plates. **a** Dynamic Mold Plates **b** Static Mold Plates

**Fig. 5** Parts made using protected CBAM mold plates



the CBAM-produced part performed most similarly to the traditional steel mold-produced part. The input specifications for manufacturing are summarized in Table 4.

It was found that with 30 s of cooling time, the parts were still pliable when ejected from the composite mold. These parts were placed between two heavy plates immediately after ejection to remove the warpage induced by the ejection process. These parts were still tested through the remainder of the study, however, more cooling time is necessary to produce solid parts upon ejection.

## 4 Experimental Testing

### 4.1 Tensile Testing

Tensile testing was conducted according to ASTM D638 [28]. Tensile specimens 6.5 inches (165.1 mm) long with a test Sect. 0.5 inches (12.7 mm) wide (see Fig. 6; Table 5) were removed from the injection molded parts and prepared for testing by drawing one tracking

**Table 4** Summary of Injection Molding Input Parameters

Parameter	Steel Mold	CBAM Mold	Unit
Tonnage	330,000 (165)	330,000 (165)	lb (tons)
Injection Pressure	1800 (12410.56)	1800 (12410.56)	Psi (kPa)
Rear Heater Temperature	465 (241)	465 (241)	°F (°C)
Mid Heater Temperature	475 (246)	475 (246)	°F (°C)
Front Heater Temperature	485 (252)	485 (252)	°F (°C)
Sprue Temperature	485 (252)	485 (252)	°F (°C)
Injection Time	6	6	s
Packing Time	3	3	s
Cooling Time	10	30–90	s

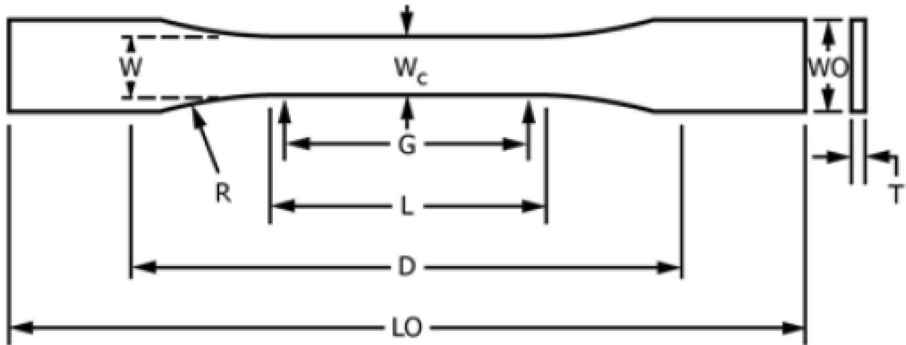


**Fig. 6** ASTM D638 Tensile Test Specimen

dot on each side of the test section. Each specimen's test section geometry was measured with calipers to the nearest 0.001 (0.0254 mm) of an inch and recorded prior to testing.

These test samples were then selected at random and loaded into an Instron 5985 universal testbed fitted with a 250kN load cell, video extensometer, and standard wedge-style tensile grips from Wyoming Test Fixtures as shown in Fig. 7. Five samples of each set were tested until failure. The extension rate was set at 1 in/min (25.4 mm/min) and data were collected at a rate of 20 Hz once the preload value of 11.2 lbf (50 N) was reached. Specimens that did not break within the ASTM allowable failure methods were discarded and not replaced.

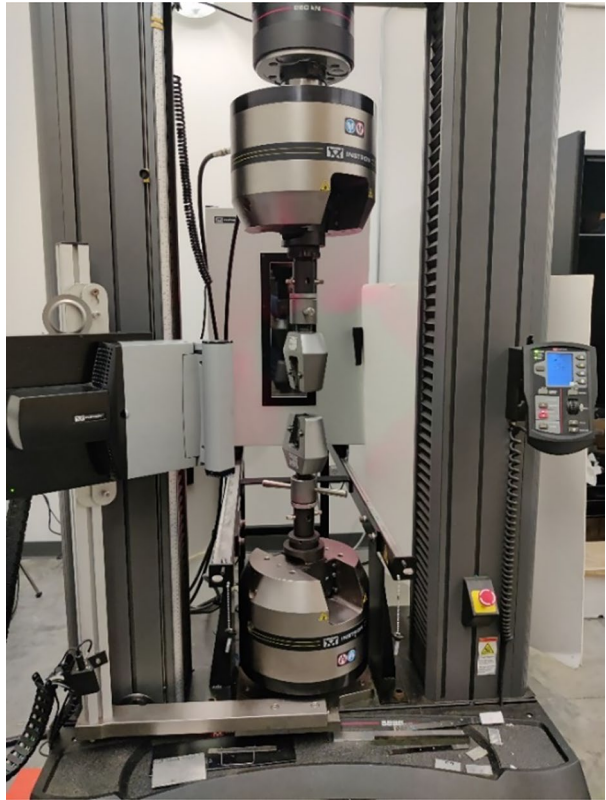
## 4.2 Flexural Testing

Flexural testing was conducted according to ASTM D790 [29]. This ASTM standard calls for 3-point flexural tests to be conducted at a strain rate of 0.01 mm/mm/min on rectangular prism-shaped specimens. Due to the part thickness being nominally 0.125 inches (3.175 mm), a 2-inch (50.8 mm) gap between supports was used for testing. Four sample sets were tested in flexure for this study: parts made in the conventional steel mold plates and cooled for 10 s, CBAM parts cooled for 30 s, CBAM parts cooled for 60 s, and CBAM parts cooled for 90 s. According to the ASTM standard, the test specimens are rectangular prisms 0.5 inches (12.7 mm) wide, 0.125 inches (3.175 mm) thick, and required to be at least 4.4 (111.6 mm) inches long. Five test specimens were selected at random from each sample set and tested until

**Table 5** ASTM D638 Tensile Test Specimen Dimensions

ASTM D638 Tensile Specimen Type 1 Dimensions	
Label	Dimension, in (mm)
W—Width of narrow section	0.50 (13)
L—Length of narrow section	2.25 (57)
WO—Width overall	0.75 (19)
LO—Length overall	6.5 (165)
G—Gage length	2.00 (50)
D—Distance between grips	4.5 (115)
R—Radius of fillet	3.00 (76)

**Fig. 7** Instron 5985 with Tensile Grips and Video Extensometer



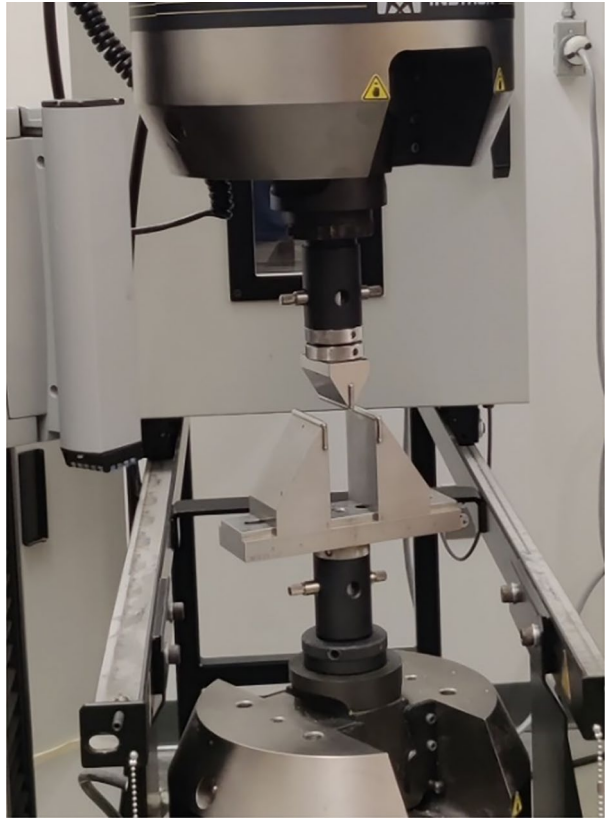
failure. The same Instron 5985 Universal Test Frame was used, this time using a Wyoming Test Fixtures three-point flexure test fixture as shown in Fig. 8.

## 5 Results and Discussion

### 5.1 Tensile Test

During the test, elongation, load, and strain data were collected at a rate of 20 Hz. This data included time, load, mechanical extension, stress, and strain as measured by the video extensometer. From this, stress-strain curves were plotted and shown in Fig. 9 below.

The data shows a very high correlation between the samples built in the steel mold and the CBAM mold. The difference in average ultimate tensile strength ( $\sigma_{ULT}$ ) is 3.74% and the difference in average elastic modulus (E) is 1.27%. These differences are minuscule and can very easily be attributed to experimental variation, thus it can be concluded that parts made in a CBAM injection mold have similar tensile properties to those made in traditional steel molds.

**Fig. 8** Flexural Test Setup

## 5.2 Flexural Test

Flexural testing was conducted with a sampling rate of 20 Hz. Five specimens per sample were utilized and the tests were run until the material failed. Each specimen was measured at the center of the test section using calipers to the nearest 0.001 inches (0.025 mm). The strain was calculated from extension and cross-sectional area. The stress and strain were then plotted in Figs. 10, 11 and 12 below.

The data generally shows good agreement between the parts made with the conventional and steel molds, especially those cooled for 60 s. From this data, the flexural modulus was calculated according to Eq. (4).

$$E_B = \frac{L^3 m}{4bd^3} \quad (4)$$

where  $E_B$  is the flexural modulus,  $L$  is the length of the support span,  $m$  is the slope of the tangent to the initial straight-line portion of the load-deflection curve,  $b$  is the width of the specimen, and  $d$  is the depth of the specimen. After testing was complete, the flexural modulus of the parts made in the steel mold was calculated and averaged. The same calculations were conducted on each set of parts from the composite molds and compared to the steel. The flexural moduli of the composite and steel molds at three different cooling times

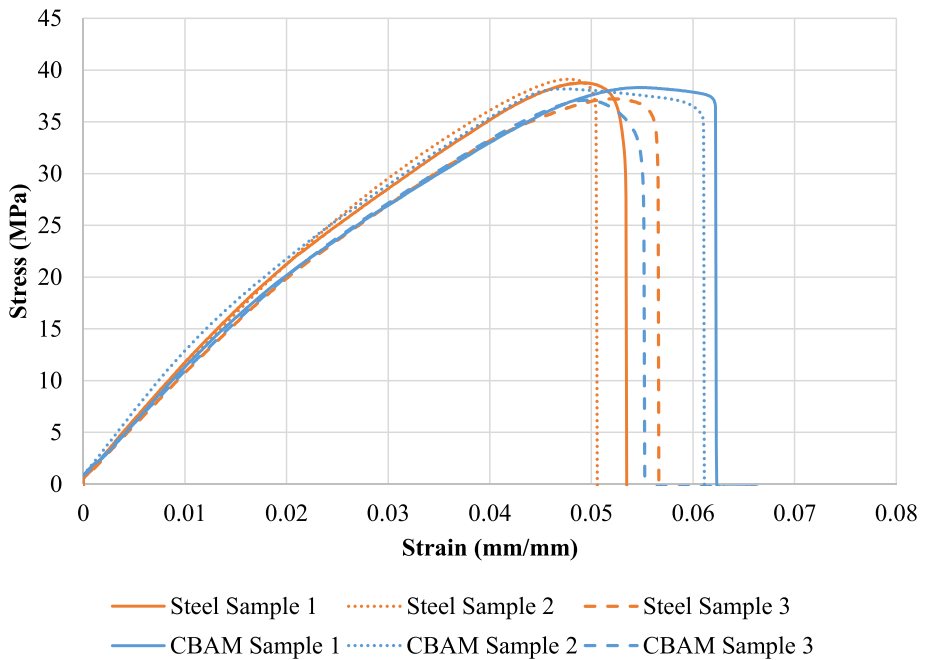


**Fig. 9** Tensile Stress-Strain Curves

are compared in Fig. 13. The ultimate flexural stresses were also compared between the steel and composite molds and are shown in Fig. 14.

The flexural testing results are very similar between the parts made in the steel mold and the composite mold. This high correlation shows that when the cooling rate is accounted for, parts made in either conventional or CBAM molds have nearly identical mechanical properties.

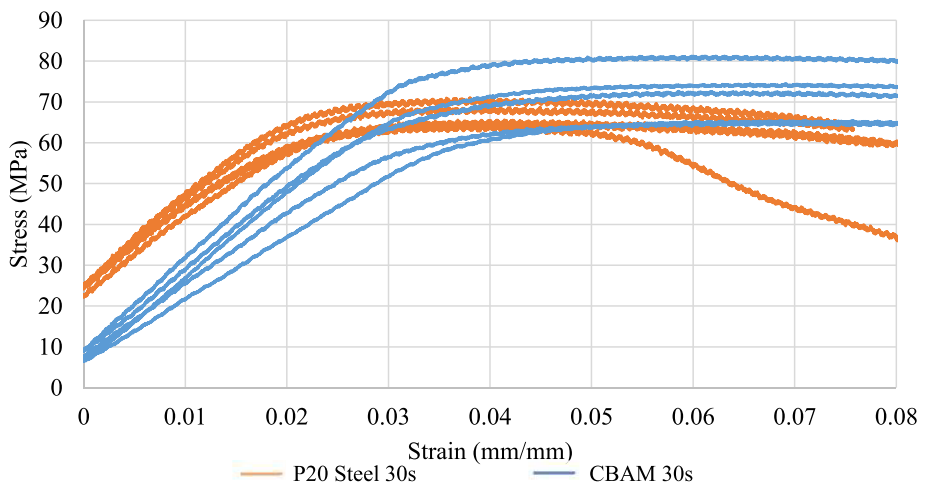


**Fig. 10** Flexural Testing Stress-Strain Curves with 30 s Cool Time

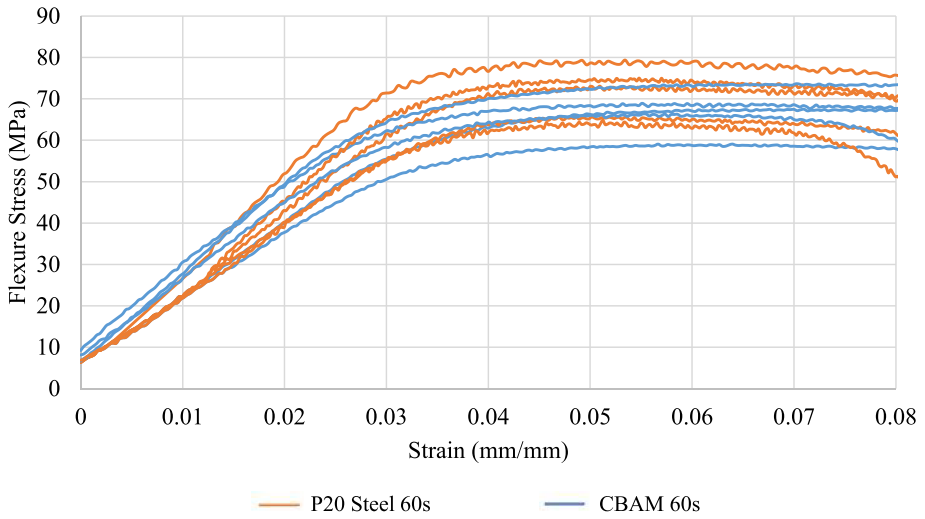


Fig. 11 Flexural Testing Stress-Strain Curves with 60 s Cool Time

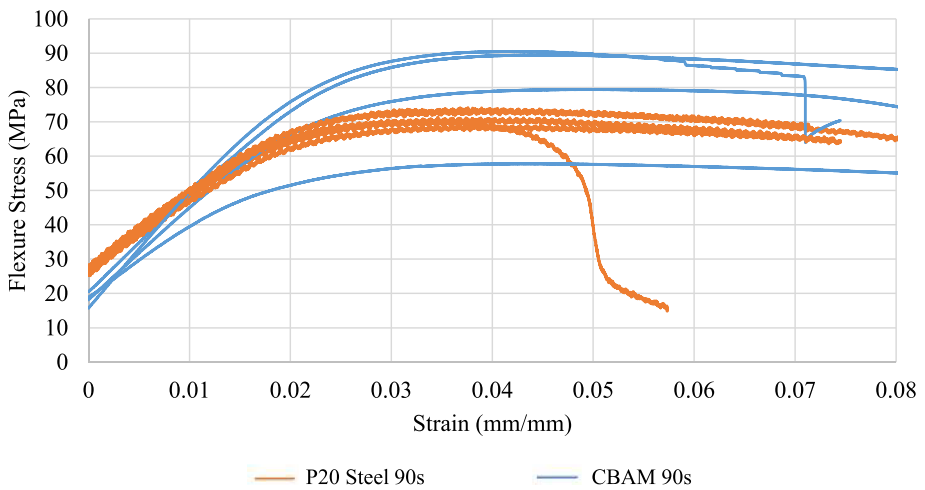
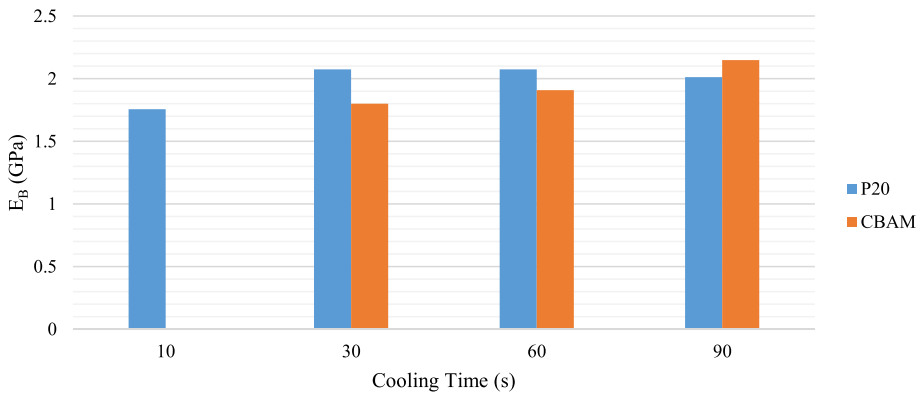
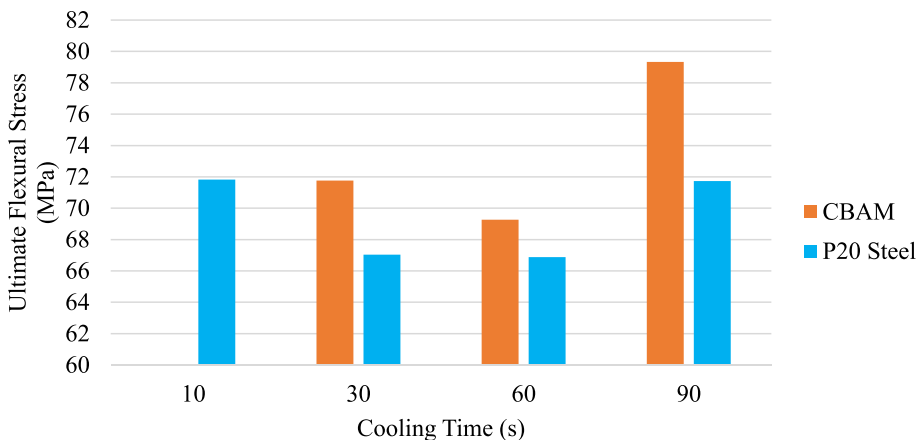


Fig. 12 Flexural Testing Stress-Strain Curves with 90 s Cool Time





**Fig. 13** Flexural Modulus of CBAM Mold Manufactured Parts Compared to Steel Mold Manufactured Parts



**Fig. 14** Average Ultimate Flexural Stress of CBAM Mold Manufactured Parts Compared to Steel Mold Manufactured Parts

## 6 Conclusions

In modern injection molding manufacturing environments, the ability to quickly change part designs is more important now than ever. Thus, new technologies for creating mold plates are being explored to reduce the minimum number of parts in a run, as well as creating more flexibility in mold designs, and vastly lowering the lead time to the first part. In this study, injection molding plates of the same design were built using two different techniques: one being conventionally CNC machined P20 stainless steel molds, and the other being composite additively manufactured molds using carbon fiber and a PEEK matrix. Parts were then manufactured in each mold using Lustran 348 ABS plastic. These parts were then tested in tensile and flexure. It was found that the tensile strength of the parts made in the composite molds was within 5% of that of the conventional mold and the flexure strength was within 10% of the conventional mold. Thus, it can be concluded that the composite mold makes an adequate substitute for the traditional steel mold. The advantages

of the composite mold are that due to its use of additive manufacturing, manufacturing lead times can be as low as 7–14 days compared to multiple months for conventional steel machining. Further, due to lower labor and material costs, the composite mold used in this study cost less than 15% of what a comparable steel mold costs. This reduces the minimum number of parts needed to be run substantially. Finally, the composite mold incorporates a weight savings of over 50% compared to the steel mold. This could be important in environments where molds are being switched out often and prototyping complex injection molded parts.

**Data Availability** The data that support the findings of this study are available from the corresponding author upon request.

## Declarations

**Competing Interests** The authors have no competing interests to declare that are relevant to the content of this article.

## References

- 2021 Plastics Industry Association Size and Impact Study. Washington DC, United States (2021)
- Fu, H., Xu, H., Liu, Y., Yang, Z., Kormakov, S., Wu, D., Sun, J.: Overview of injection molding technology for processing polymers and their composites. *ES Mater. Manuf.* **8**(3), 3–23 (2020). <https://doi.org/10.30919/esmm5f713>
- Rosato, D., Rosato, D., Rosato, M.G.: The complete injection molding process. In: *Injection Molding Handbook*, pp. 1–27. Springer Science + Business Media, New York (2012)
- Zheng, R., Tanner, R.I., Fan, X.-J.: Introduction and rheology. In: *Injection molding: integration of theory and modeling methods*, pp. 1–35. Springer, Berlin (2011)
- Kazmer, D.O.: Mold cost estimation. In: *Injection Mold Design Engineering*, pp. 43–77. Hanser Publications, Cincinnati, OH (2016)
- Bogaerts, L., Faes, M., Bergen, J., Cloots, J., Vasiliauskaite, E., Vogeler, F., Moens, D.: Influence of thermo-mechanical loads on the lifetime of plastic inserts for injection moulds produced via additive manufacturing. *Procedia CIRP*. **96**, 109–114 (2021). <https://doi.org/10.1016/J.PROCIR.2021.01.061>
- Lozano, A.B., Álvarez, S.H., Isaza, C.V., Montealegre-Rubio, W.: Analysis and advances in additive manufacturing as a new technology to make polymer injection molds for World-Class Production Systems. *Polymers* **14**(9), 1646 (2022). <https://doi.org/10.3390/POLYM14091646>
- Dizon, J.R.C., Valino, A.D., Souza, L.R., Espera, A.H., Chen, Q., Advincula, R.C.: 3D printed injection molds using various 3D printing technologies. *Mater. Sci. Forum.* **1005**, 150–156 (2020). <https://doi.org/10.4028/WWW.SCIENTIFIC.NET/MSF.1005.150>
- Gohn, A.M., Brown, D., Mendis, G., Forster, S., Rudd, N., Giles, M.: Mold inserts for injection molding prototype applications fabricated via material extrusion Additive Manufacturing. *Additive Manuf.* **51**, 102595 (2022). <https://doi.org/10.1016/J.ADDMA.2022.102595>
- Krizsma, S., Kovács, N.K., Kovács, J.G., Suplicz, A.: In-Situ monitoring of deformation in rapid prototyped injection molds. *Additive Manuf.* **42**, 102001 (2021). <https://doi.org/10.1016/J.ADDMA.2021.102001>
- Jahan, S., Wu, T., Shin, Y., Tovar, A., El-Mounayri, H.: Thermo-Fluid Topology optimization and experimental study of conformal cooling channels for 3D printed plastic injection molds. *Procedia Manuf.* **34**, 631–639 (2019). <https://doi.org/10.1016/J.PROMFG.2019.06.120>
- Agarwal, B.D., Broutman, L.J., Chanshekhara, K.: Introduction. In: *Analysis and performance of fiber composites*, pp. 1–16. John Wiley & Sons (2017)
- Composite-Based 3D Printing for Industrial Manufacturing: Impossible objects. <https://www.impossible-objects.com/industry-industrial-manufacturing/>. Accessed 18 Jun 2022
- Impossible Objects, CBAM-2: <https://www.impossible-objects.com/cbam-printer/>. Accessed 10 May 2022
- Impossible Objects ASTM E831 CTE Testing: Winnipeg (2017)
- Impossible Objects: ASTM D5470 Thermal Transmission Testing Report: Winnipeg (2017)

17. Ricoh, and Impossible Objects: Printing the impossible. Stevenage (2022)
18. Sanei, S.H.R., Popescu, D.: 3D-printed carbon fiber reinforced polymer composites: A systematic review. *J. Compos. Sci.* **4**(3), 98 (2020). <https://doi.org/10.3390/JCS4030098>
19. AISI Type P20 Mold Steel (UNS T51620): <https://www.matweb.com/search/datasheet.aspx?matguid=2957f352a2e84857a9c41d2f31d063ec&ckck=1>. Accessed May 12, 2022
20. Lustran 348: INEOS Styrolution. [https://www.ineos-styrolution.com/Product/-\\_Lustran-348\\_SKU401200371209.html](https://www.ineos-styrolution.com/Product/-_Lustran-348_SKU401200371209.html). Accessed 10 May 2022
21. Lustran 348 WT SDS: Aurora (2020)
22. Vates, U.K., Kanu, N.J., Gupta, E., Singh, G.K., Daniel, N.A., Sharma, B.P.: “Optimization of FDM 3D printing process parameters on ABS based bone hammer using RSM technique”. *IOP Conf. Ser. Mater. Sci. Eng.* **1206**(1), (2021). <https://doi.org/10.1088/1757-899X/1206/1/012001>
23. A Detailed Guide on Acrylonitrile Butadiene Styrene: SpecialChem. <https://omnexus.specialchem.com/selection-guide/acrylonitrile-butadiene-styrene-abs-plastic>. Accessed 10 May 2022
24. Park, S.J., Kwon, T.H.: Optimal cooling system design for the injection molding process. *Polym. Eng. Sci.* **38**(9), 1450–1462 (1998). <https://doi.org/10.1002/PEN.10316>
25. Yang, Y., Chen, X., Lu, N., Gao, F.: Injection molding process control, monitoring, and optimization. Hanser Publications, Cincinnati (2016)
26. Menges, G., Michaeli, W., Mohren, P.: How to make injection molds. Hanser Publishers, Cincinnati (2001)
27. Bivens, C.M.: Composite-based additive manufacturing applications in the polymer injection molding cycle. Rolla (2021)
28. “ASTM D638-14: Standard test method for tensile properties of plastics. ASTM Int. (2014). <https://doi.org/10.1520/D0638-14>
29. “ASTM D790-17: Standard test methods for flexural properties of unreinforced and reinforced plastics and electrical insulating materials. ASTM Int. (2017). <https://doi.org/10.1520/D0790-17>

**Publisher’s Note** Springer Nature remains neutral with regard to jurisdictional claims in published maps and institutional affiliations.

Springer Nature or its licensor (e.g. a society or other partner) holds exclusive rights to this article under a publishing agreement with the author(s) or other rightsholder(s); author self-archiving of the accepted manuscript version of this article is solely governed by the terms of such publishing agreement and applicable law.